CONCRETE LIBRARY OF JSCE NO. 22, DECEMBER 1993

TRIAXIAL ELASTO-PLASTIC AND CONTINUUM FRACTURE MODEL FOR CONCRETE



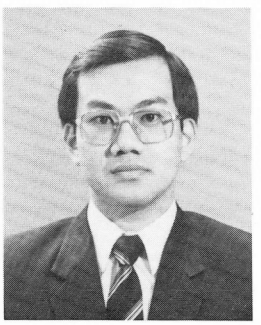
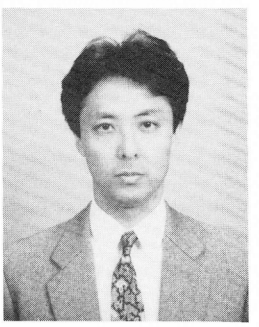

Koichi MAEKAWA Jun-ichi TAKEMURA Paulus IRAWAN Masa-aki IRIE

SYNOPSIS

Complete constitutive equations in the form of a tangential stiffness matrix are derived by incorporating the constitutive law of continuum fracturing with the one for plasticity. Triaxial stress states are the main concern of the authors since the wish is for the model to be a crucial and universal tool of analysis for laterally confined reinforced concrete columns with a wide variety of geometries and dimensions. The constitutive equation derived under triaxial stresses was proven to cover the plastic and fracturing characteristics of concrete as well as the Von-Mises type of plasticity which serves as a model of steel in reinforced concrete. The authors validated the fitness of the model for the triaxial behavior of concrete. The failure envelope is not explicitly utilized in the formulation, in contrast to the theory of plasticity, but it can be computed as a result of evolution of simultaneous fracturing and plasticity.

Keywords : *constitutive law, fracture, damage mechanics, plasticity, dilatancy, confinement*

K. Maekawa is Associate Professor of Department of Civil Engineering, The University of Tokyo, Tokyo, Japan. His research interest covers reinforced concrete mechanics, computational approach to seismic behaviors of RC-Soil system, thermodynamics of cement-concrete composite, and durability design of concrete structures.

J. Takemura serves as an official for Japan Ministry of Transportation, and was a former graduate student of The University of Tokyo, Tokyo, Japan.

P. Irawan is a graduate student in Department of Civil Engineering, The University of Tokyo, Tokyo, Japan. His research is in the mechanical behaviors of concrete under triaxial confinement.

M. Irie is a civil engineer of Nikken Sekkein Co. Ltd., Tokyo, Japan and was a former graduate student of The University of Tokyo, Tokyo, Japan.

---

1. INTRODUCTION

The source of concrete non-linearities generally can be traced to continuum fracture and plasticity. Continuum fracture is defined as the elasticity damage sustained in absorbing and releasing the elastic strain energy caused by an assembly of spatially dispersed defects with no distinguishable localization [1]. On the other hand, plasticity is defined as the unrecoverable deformation of concrete after all stresses applied to it have been removed. In general, continuum fracture will affect strength and plasticity will influence the ductility of concrete. The concept of combined elasto-plasticity and fracturing, which has been developed for the two-dimensional problem of concrete panels [1], is extended to three-dimensional problems such as the behavior of concrete under triaxial confinement.

A schematic outline of an elasto-plasticity and fracturing system can be seen in Fig.1. Concrete is regarded as a set of infinitesimal elasto-plastic components. Concrete elasticity is represented as parallel springs and the plasticity is modelled by a dashpot. Broken springs are used to indicate damage in the concrete. The total stress in the concrete can be regarded as the summation of the contribution made by the internal stress in each non-damaged element of the constituents. From Fig.1, it can be seen that for elasto-plastic materials, the elastic strain is proportional to the internal stress intensity applied to non-damaged components.

Figure 2 shows the complete scheme of the elasto-plastic fracture concept, as used to formulate the constitutive laws of concrete under triaxial stresses. Unlike the common formulation of damage and plasticity based on total stress or strain, the concept of internal stress, which is directly proportional to the elastic strain, was adopted for the evaluation of stress intensity applied to the non-damaged volume, which retains the capacity to absorb and release elastic strain energy.

As shown in Fig.2, our discussion is divided into three main parts, a consideration of continuum fracturing and plasticity in concrete nonlinearities under triaxial confinement and the combination of these two factors to form a complete constitutive law. In the first part, the effect of damage occuring in the concrete on the relationship between internal stress intensity - represented by elasticity - and total stress is the topic of discussion. In the next part, plasticity will be discussed in terms of elasticity and concrete damage. Finally, by applying the compatibility condition, the relationship between total stress and total deformation can be obtained.

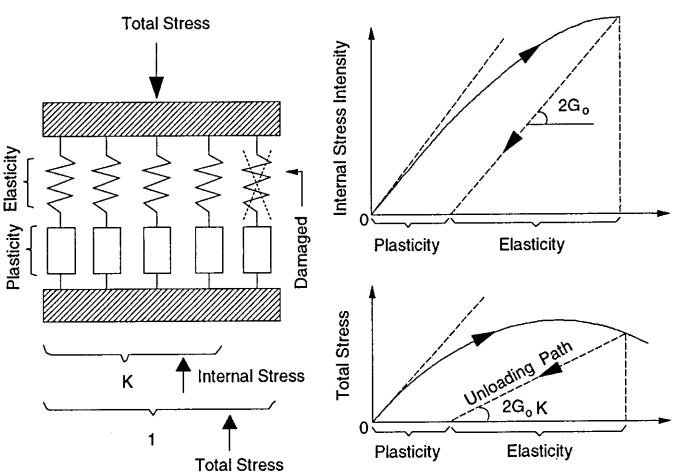

Fig.1 Schematic Outline of Elasto-Plasticity and Fracturing System

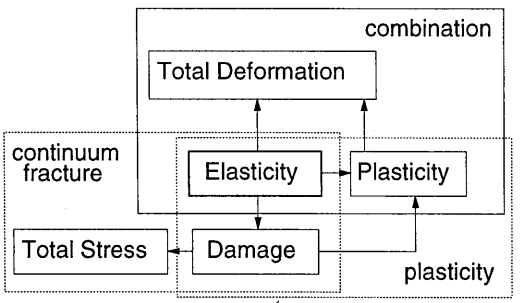

Fig.2 Scheme of Formulation within the Framework of the Elasto-Plasticity and Fracturing Concept

2. CONTINUUM FRACTURE IN CONCRETE NONLINEARITY UNDER TRIAXIAL CONFINEMENT

2.1 General

The effect of three-dimensional (3D) confinement on strength and ductility has been reported worldwide, and the overall nonlinearity of the problem has been of main concern. This chapter aims at a general constitutive law for predicting continuum fractures appearing in concrete nonlinearities under 3D generic stresses. The key to this chapter is the extraction of continuum fractures from the many nonlinearities occurring under triaxial stress. It is shown that mechanics of the extracted continuum fracture can be simply described by this constitutive law even though the 3D nonlinearities of concrete regarded as a combination of plasticity and fracturing seem complex as a whole [1]. The total energy absorbed by the concrete should be estimated with regard to the plastic and frictional energy converted to heat as well as the fracture energy used to generate cracks and defects.

In this study, the volumetric (mean) and deviator components of damage elasticity are individually discussed. A quantification of deteriorated elastic energy absorption is sought under triaxial stress states. The so called "*confinement effect*", used vaguely in the past, is strictly defined as the effect of the hydrostatic component of triaxial internal stress on the damage elasticity.

The continuum fracture model discussed in this chapter is thought to act as one component in the complete system of elasto-plasticity and fracturing constitutive laws as shown in Fig.2. Thus, the total stress has to be mathematically related to the elasticity, which represents the intensity of internal stress [1] and the damage condition predicted in terms of the continuum fracture. The plasticity of the damaged continuum must be incorporated along with the continuum fracture into the overall formulation scheme as illustrated in Fig.2. As far as the plasticity appearing in 3D nonlinearities is concerned, close attention will be paid to it in the next chapter.

2.2 Coverage of Loading Path

Typical paths of 3D loading tests conducted in past research were summarized by Mang, et al. [8] in terms of the hydrostatic and deviator invariants of total stresses, denoted by I_1 and J_2 (see Fig.3), as,

$$I_1 = \frac{1}{3}\sigma_{ii} \tag{1a}$$

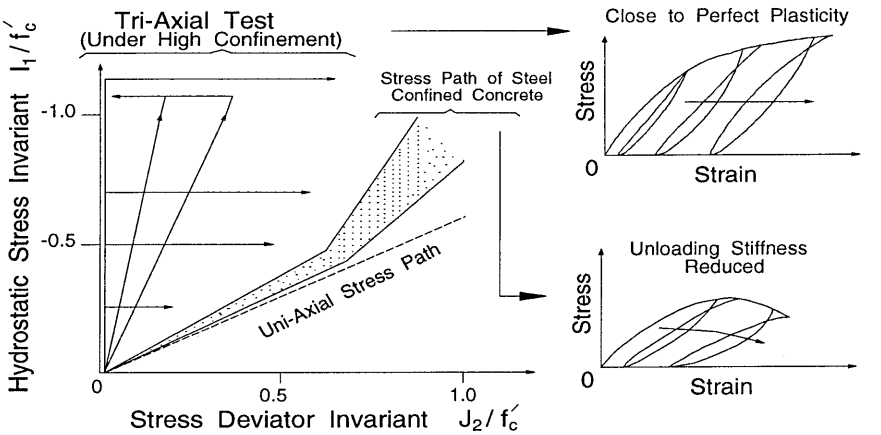

Fig.3 Stress Path to be Covered and Corresponding Nonlinearity

$$J_2 = \sqrt{\frac{1}{2} s_{ij} s_{ij}} \tag{1b}$$

$$s_{ij} = \sigma_{ij} - \delta_{ij} I_1 \tag{1c}$$

where, σ_{ij} and s_{ij} are the total stress and stress deviator tensors, respectively, and positive values express tension. If there is a [′] (prime) mark, the rule of sign is reversed, i.e., compression is defined as positive. This inverse rule holds for strain and its invariants, too. The compressive strength of concrete is denoted by f_c', which is positive definite.

In general, the hydrostatic invariant I_1, the indicator of confinement, is much greater than that of the deviator in a comparison of the loading conditions adopted in specimen based tests with typical stress states occurring in RC columns with lateral steel. In Fig.3, where typical loading paths of triaxial tests conducted in the past are shown, it should be noted that the confinement happens to be so great that the unloading stiffness remains unchanged. This means that elasticity seems not to deteriorate. On the contrary, the smaller the hydrostatic invariant, a much greater reduction in unloading stiffness proceeds irreversibly [5]. The reduction of the unloading stiffness, which is specified as the damage elasticity, is the mark of continuum fracturing. It can be qualitatively said that fracturing is associated with confinement.

Since the actual lateral reinforcement of columns gives rise to a lesser hydrostatic invariant in the core concrete, the quantification of the continuum fracturing as well as plasticity is assumed to be indispensable for the purposes of structural analyses of capacity and ductility gain. The authors concentrated on the continuum fracturing of elasticity applicable to relatively higher deviatoric and lower hydrostatic stress states.

2.3 Separation of Elasticity from Damaged Concrete

Figure 4 shows the axial stress-strain relation for cylinder specimens confined by steel rings, which supply the lateral normal stress in concrete by self-equilibrium. Since the rings were uniformly distributed, the lateral stress when the steel reaches yield is equal to $\rho f_y/2$, where ρ is the volume ratio of steel and f_y is the yield strength of the steel rings. In the tests, the lateral stress at the yield point ranged from 0MPa to 12MPa. The axial load was applied through teflon sheets to reduce frictional confinement applied by the testing machine [5,10].

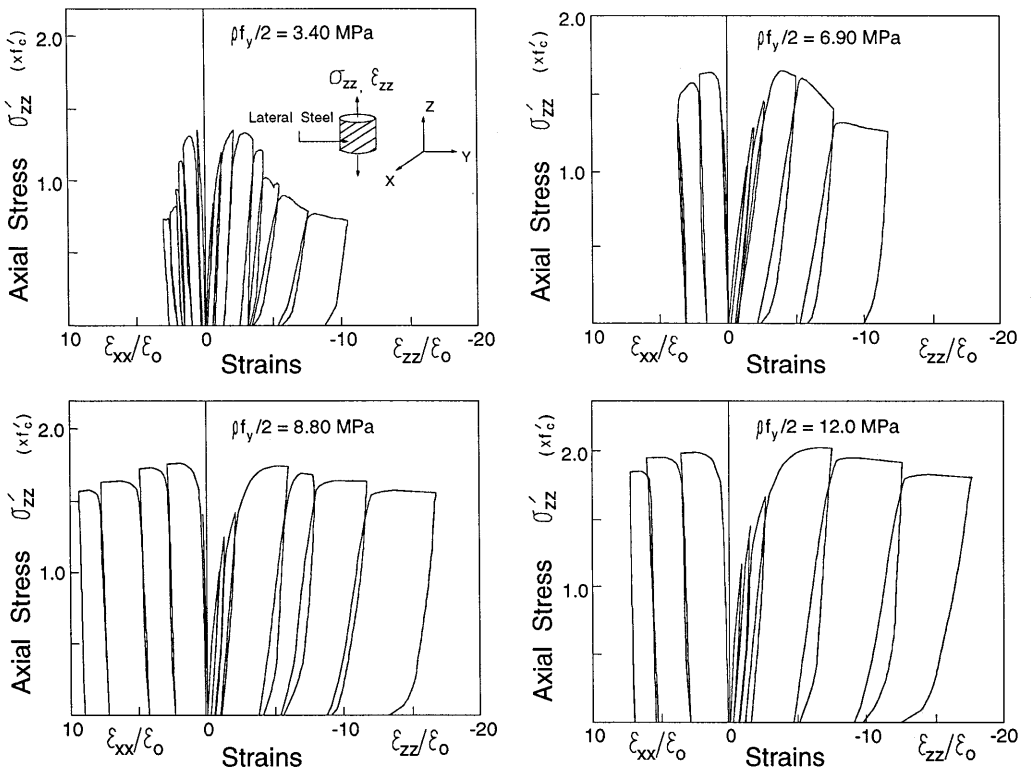

Fig.4 Stress-Strain Relation of Steel-Confined Cylinder : f_c' =29MPa, $\varepsilon_o = 0.0025$

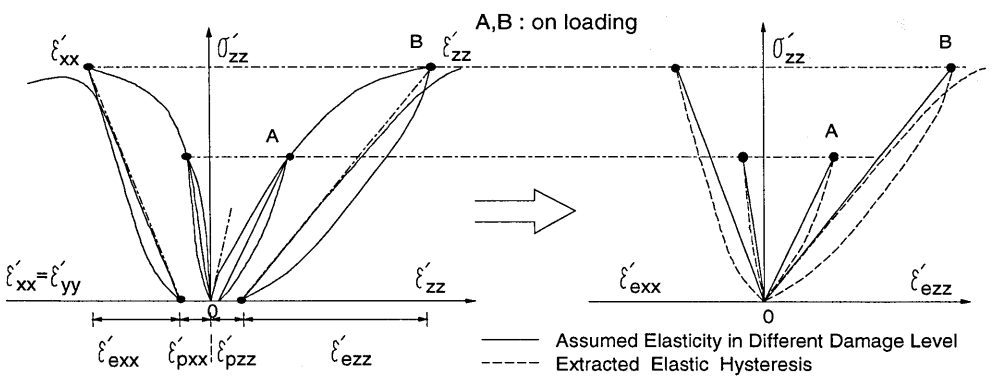

Fig.5 Separation of Elasticity and Plasticity through Experiments

The authors define the plastic strain tensor ε_{pij} as the residual total when the stress is completely removed, as shown in Fig.5. The rest of the total strain associated with acting stresses is defined as the elastic strain ε_{eij}, and is the component of interest to us. For example, when we implement complete unloading from point A or B in Fig.5, the axial and lateral elastic strains denoted by ε'_{ezz}, ε'_{exx}, and ε'_{eyy} can be obtained. At the

same time, by using Eq.(1), we can compute the stress invariants corresponding to the point A or B, as appropriate. Thus, it is possible to get several data sets for elasticity and the updated stress at different intensities by conducting cyclic 3D loading tests on concrete.

$$\varepsilon_{eij} = \varepsilon_{ij} - \varepsilon_{pij} \tag{2}$$

The elasto-volumetric first invariant, and the deviator second and third invariants $<I_{1e}, J_{2e}, J_{3e}>$ can be defined in the same manner as the stresses on the loading envelopes (see Fig.5) as,

$$I_{1e} = \frac{1}{3}\varepsilon_{eii} \tag{3a}$$

$$J_{2e} = \sqrt{\frac{1}{2}e_{eij}e_{eij}} \tag{3b}$$

$$J_{3e} = \sqrt[3]{\frac{1}{3}e_{eij}e_{ejk}e_{eki}} \tag{3c}$$

where, e_{eij} (= ε_{eij} - δ_{ij} I_{1e}) is the elastic deviator tensor. Tension is also defined as positive here and the [′] means the sign rule is reversed.

Damage mechanics as proposed in the past were mainly coupled with the total strain and stress relation [6]. The residual strain upon complete stress release is computed in terms of the inelastic stresses [11,12,13]. However, the authors attempt to relate the elasticity of damaged concrete with the path of the total stresses. It is expected that the combination of plasticity described independently from the continuum fracture concerned will yield the full constitutive laws [1]. The elasticity defined above is still cyclic stress-path dependent in the same way as plasticity (see Fig.5). In this paper, we try first to explain the continuum fractures occurring in elasticity of the loading condition. Concerning cyclic nonlinearities, the multi-component modeling of elasto-plasticity and fracturing done by Song and Maekawa [3] will be applied in future.

So far, few tensorial discussions of the continuum fractures have been carried out for 3D generic states. Mazars [11], Simo [12] and Schreyer [13] proposed tensorial forms of the damaged continuum. Due to the complete isotropy of the stiffness matrix derived, Poisson's ratio for unloading is automatically the same as the initial value. However, damaged concrete exhibits a varying Poisson's ratio under the elastic response [1]. This experimental reality implies non-associated damage accumulation (anisotropy of fracturing). The authors will pay special attention to the volumetric and deviatoric aspects of continuum damage in concrete. If the rate of fracture energy release is different (non-associated) in the volumetric and deviatoric modes, the apparent Poisson's effect at least differs from the initial value. This will be one of the primary discussions in this chapter.

2.4 Volumetric Elasticity and Fracture

The stiffness of the separated elastic strain-versus-stress relation is known to vary according to the loading path under biaxial stresses [1]. We have the same situation also under the triaxial stress state shown in Fig.4 [5]. We first tried to pick up the fracture arising in the volumetric component of elasticity.

The hydrostatic stress and volumetric elastic strain invariants are plotted in Fig.6, where the different levels of confinement by steel shown in Fig.4 are brought together. The lateral stress on the loading path acts on the circular section of the cylinders isotropically. The results shown in Fig.6 appear meaningful to us. Regardless of the different confinement, denoted by I_1, on the loading path, no continuum fracturing is observed in the volumetric mode of elasticity when the applied hydrostatic stress is less than 0.5 f_c'.

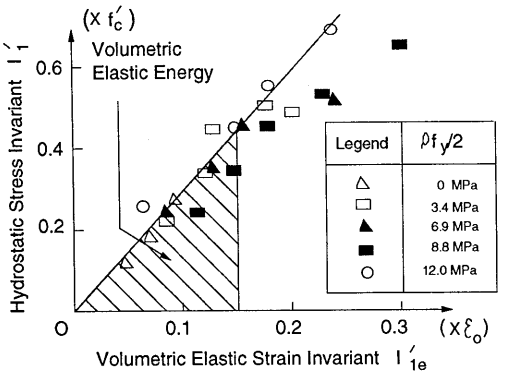

Fig.6 Relationship of Hydrostatic Stress versus Volumetric Elasticity

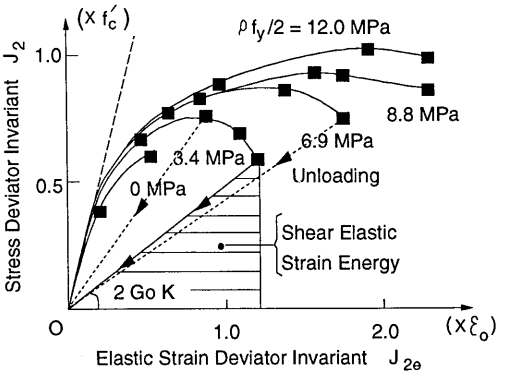

Fig.7 Relationship of Deviator Stress-versus-Strain Invariants

The area enclosed by I_1 and I_{1e} represents the reversible hydrostatic energy of the damaged concrete including defects and cracks. The density of the microscopic defects might be different in each specimen due to different levels of lateral stress, but the hydrostatic energy absorption capacity remains unchanged and undamaged when applied hydrostatic stress is less than $0.5 f_c'$. In other words, the entire volume of concrete effectively absorbs and releases hydrostatic component of elastic strain energy.

Under higher hydrostatic stress, damage in the volumetric mode is seen, but the reduction in volumetric stiffness is within 20% and the inelastic volumetric strain is less than $0.09\varepsilon_o$. This means that if we neglect the volumetric nonlinearity of fracturing, the error in predictions of normal strain is around $0.03\varepsilon_o$. Since the authors intend to apply the continuum fracture model to steel-confined concrete in which the stress deviator invariant is prominent (see Fig.3), it may be acceptable to assume no fracturing in the volumetric mode. Therefore, the constitutive law of volumetric elasticity takes the same form as the linear elasticity, that is:

$$I_1 = 3K_o I_{1e} \tag{4}$$

The constant K_o is the volumetric elasticity constant equal to $E_o/3(1-2\nu_o)$, where E_o and ν_o are elastic Young's module and Poisson's ratio. These values can be obtained from the initial stiffness.

2.5 Elastic Deviator and Fracturing

(1) Deteriorated Shear Elasticity

Figure 7 shows the stress and elastic strain deviator invariants at each loading with different levels of lateral confinement. When the load is removed, the stress and elastic strain go back to the origin according to the definition. The higher the lateral confinement on the concrete, the more the stress deviator invariant is sustained by the damaged concrete. Here, according to the analogy of the elasto-plastic and fracture models [1], the fracture parameter K can be written in terms of the stress and elastic strain deviator invariants as,

$$J_2 = 2G_o K J_{2e} \tag{5}$$

where, G_o is the elastic shear modulus which coincides with the initial shear stiffness, and is equal to $E_o/2(1+\nu_o)$. Accordingly, the value of K is positive definite and not greater than unity.

The area enclosed by a line connecting point <0,0> and point <J_2, J_{2e}> and its projection to J_{2e} axis as shown in Fig.7 corresponds to shear elastic strain energy stored in concrete. The lower confinement reduces the capacity to store shear elastic strain energy. The area enclosed by J_2-J_{2e} curve and its projection to J_{2e} axis minus the shear elastic strain energy represents the fracture energy consumed by the generation of defects in concrete. The value of K indicates the ratio of effective concrete volume which can absorb and release the shear elastic strain energy, and (1-K) implies the loss of concrete volume to absorb and release this energy.

(2) Fracture parameter

Let us again consider the elasto-plastic and fracture system consisting of parallel springs, as shown in Fig.2. Since the value of K represents the remaining volume of concrete with non-damaged shear elasticity, it can be treated as the ratio of remaining springs sustaining shear stress. From this analogy, we can write the internal stress intensity denoted by J_{2i} on the active springs in Fig.2 as,

$$J_{2i} = \frac{J_2}{K} = 2G_o J_{2e} \tag{6}$$

To predict fractures, the total stress J_2 is not appropriate because J_2 does not represent the internal stress intensity arising in the effective constituent element. Since J_{2e} is directly proportional to J_{2i}, it implicitly represents the internal shear intensity applied to the "*effective volume*". The authors adopted elasticity as an indicator to represent the magnitude of internal stress applied to an effectively non-damaged part of the damaged continuum concerned. Fracturing and plasticity should be described by the internal stress. The internal stress is greater when a smaller fracture parameter is assumed even if a lower total stress is applied.

The progress of continuum fracturing has been proven only in the shear mode. According to Eq.(4) and similarly to Eq.(6), I_{1e} also represents the confinement in terms of the internal stress intensity, which is expected to restrain the progress of the fracture. The authors adopted the elastic strain invariants as parameters to predict the value of K to indicate continuum fracturing.

Figure 8 shows the progress of continuum fracturing when the shear elastic intensity is increased. The confinement described by the volumetric invariant is not constant during the loading process, but has a different level in each test. A higher confinement is shown to restrain the evolution of fracturing by increasing the deviator invariant. From cyclic loading tests of confined cylinders, such as those reported by Ohshima [5] and Irie et al. [10], we have a number of data sets <I_{1e}, J_{2e}, K> covering the loading path as explained in Section 2.3 (see Fig.5).

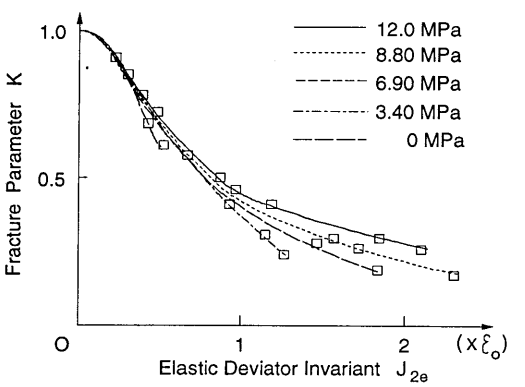

Fig.8 Fracture Evolution under Different Confinements

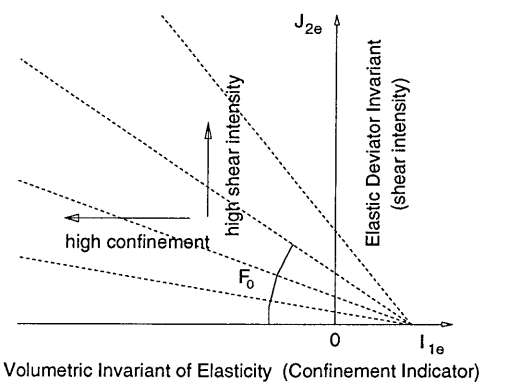

Fig.9 Influences on Continuum Fracturing

Let us first discuss the effect of I_{1e} and J_{2e} on fracturing. As shown in Fig.8, a higher internal shear intensity accelerates the evolution of fracturing but a higher confinement restrains fracturing. There is contour lines on the plane $<I_{1e}, J_{2e}>$ representing constant values of fracture parameter K. The authors assumed linear contour lines, as shown in Fig.9, where each line can be specified by its gradient. The equivalent elastic strain, denoted by F_o was defined from Fig.9, thus defining the fracture criterion. The value of F_o indicates the equivalent elasticity level at which common fractures occur. We propose the following empirical formula, which yields the following unique relation between the fracture parameter and the value of F_o:

$$F_o = \frac{\sqrt{2}J_{2e}}{0.23\varepsilon_o - \sqrt{3}I_{1e}} \tag{7a}$$

$$\varepsilon_o = 1.6(1+\nu_o)\frac{f_c'}{E_o} \tag{7b}$$

where, f_c' is the uniaxial compressive strength and ε_o is a material constant obtained such that Eq.(7a) is applicable to compressive strength of concrete from 15MPa to 50MPa [5,10]. In the tensorial expression [4], the term $\sqrt{2}J_{2e}$ geometrically represents the arch length of the π-plane, and $\sqrt{3}I_{1e}$ corresponds to the location of the π-plane measured from the origin (see Fig.11).

The continuum fracturing discussed above is conceptually formed within compression. But, in fact, the isotropic tension can be carried by concrete without any catastrophic fracture when the applied shear is small. Thus, as regards progressive fracturing, the bottom term of Eq.(7) is introduced as an indicator of the effective compressive confinement originated from the critical isotropic tension denoted by material constant $0.23\varepsilon_o$, which also indicates the tensile coordinate of the focal point as shown in Fig.9. Equation (7) has not been verified for the case of high-strength or lightweight concrete, in which the coarse aggregate is split and damaged sharply by local tension, unlike the normal concrete.

As far as the steel-encased confinement is concerned, a unique relationship between the fracture parameter and equivalent strain exists regardless of the confinement, as shown in Fig.10. In order to verify the versatility of the fracture parameter, the authors conducted cyclic biaxial compression tests in accordance with the procedure specified in reference [1]. However, the fracture parameter can not be well predicted by the same line when the isotropic biaxial compression path is adopted, and the source of this discrepancy has to be taken into account.

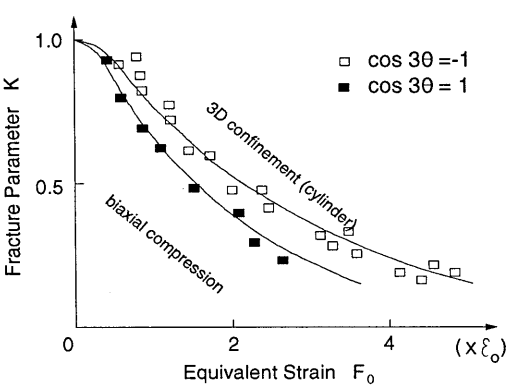

Fig.10 Relationship between Fracture Parameter and Equivalent Strain

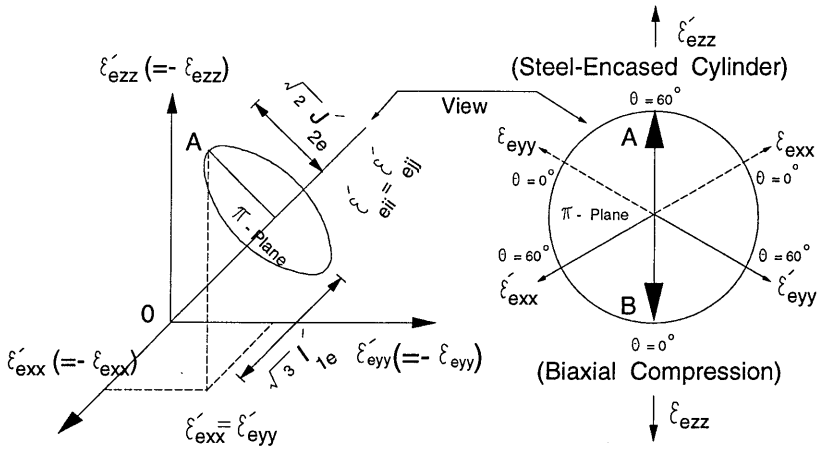

Fig.11 Elastic Strain State on the π-Plane under Common Hydrostatic and Deviator Invariants

Let us consider a plane where the values of I_{1e} and J_{2e} are common. In general, this plane is named the π-plane as shown in Fig.11. The location corresponding to the updated stress on this plane is specified by the orientation θ of the elastic deviator vector on the π-plane (see Fig.11), and is computed from the second and third invariants [4] as,

$$\cos 3\theta = \frac{3\sqrt{3}}{2}\left(\frac{J_{3e}}{J_{2e}}\right)^3 \tag{8}$$

The equivalent elasticity in the case of lateral steel confinement must be recognized as being under the special condition where the cosine of angle 3θ on the π-plane is minus unity. Another extreme case is the cyclic and isotropic biaxial compression test, in which the direction of the elastic deviator vector on the π-plane is exactly opposite of that in the steel-encased cylinder tests (see Fig.11). In this case, the value of direction cosine 3θ becomes unity. Compared with isotropic lateral confinement by a cylinder, continuum fracturing is greatly accelerated as shown in Fig.10 when a biaxial compression stress state exists. This is thought to be the effect of the third invariant. Actually, the failure envelope on the π-plane of the total stress field is not circular but distorted [4,8].

When cos3θ=-1, passive lateral confinement is realized and the fracturing is thought to be induced by the maximum principal stress. When cos3θ=1, fracturing is mainly induced by lateral action and the principal direction of the defects is different, as in the case of biaxial compression. Concerning the intermediate condition on the π-plane (-1<cos3θ<1), the authors simply and linearly assume the equivalent elasticity function F as,

$$F = F(I_{1e}, J_{2e}, J_{3e}) = F_o(I_{1e}, J_{2e})\left(\frac{6+\cos 3\theta}{5}\right) \tag{9}$$

When this value of F is adopted, we have a unique relation between the value of K and F as the 3D equivalent elastic strain as shown in Fig.12. When cos3θ=-1, the value of F coincides with F_o. Within a certain range of applicability - normal aggregate concrete, f_c'=15-50MPa -, the authors propose the following empirical equation to fit the data shown in Fig.12.

$$K = \exp\left[-\frac{F}{a}\left\{1-\exp\left(-\frac{F}{b}\right)\right\}\right] \tag{10}$$

where, F is implicitly equal to F_{max}, i.e., the maximum value of the equivalent elasticity F in past loading. If F is not equal to F_{max}, no fracturing is assumed as the damage criterion. The material constants <a, b> are empirically <3.25, 0.8>.

2.6 Tensorial Expression of Fractured Elasticity

Fracture parameter is thought to be an averaged scalar to reflect damage in concrete. The anisotropy of the reduced elasticity due to fracturing is to be considered. Li et al. [2] reported that the principal direction of the total stress coincides with that of the elastic strain even under a rotating principal axis of biaxial stresses. If coincidence is accepted, the generalized expression of the fracture elasticity is to be described as,

$$s_{ij} = 2G_o K_{ij} e_{eij} \tag{11}$$

Maekawa [1] and Li [2] also experimentally clarified the isotropy of the concrete shear elasticity under biaxial compression-tension stress. Assuming that 3D compressive stresses would make the internal damage more isotropic, the authors adopt the following tensorial expression in terms of the fractured elastic body in shear component:

$$K_{ij} = K \tag{12}$$

It can be mathematically proven that Eq.(11) and Eq.(12) satisfy Eq.(5). The isotropy in deviator tensors mentioned above holds for the fracture elasticity of concrete in shear component only. It does not mean an apparent anisotropy of concrete nonlinearities [1] caused by the overall plasticity. Combining the volumetric and deviatoric fracture laws of concrete gives the total tensorial expression for the fracture elasticity:

$$\sigma_{ij} = \delta_{ij} I_1 + s_{ij} = 3K_o I_{1e} \delta_{ij} + 2G_o K(F) e_{eij} \tag{13}$$

If the value of K is unity, Eq.(13) becomes the perfect elasticity equation. When K is hypothetically made equal to 0, Eq.(13) describes a non-frictional fluid material. Here, we have the fracture criterion where F_{max}=F and dF>0. Otherwise, the progress of the fracture is zero. Then, the incremental form of the damaging elasticity in progress is formulated as,

$$\begin{aligned} d\sigma_{ij} &= dI_1 \delta_{ij} + ds_{ij} \\ &= 3K_o \delta_{ij} d(\varepsilon_{ell}/3) + 2G_o K de_{eij} + 2G_o e_{eij} dK \\ &= M_{ijkl} d\varepsilon_{ekl} \end{aligned} \tag{14a}$$

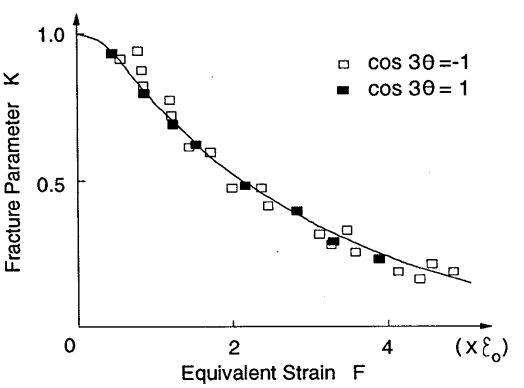

Fig.12 Fracture Parameter and Generic Equivalent Strain

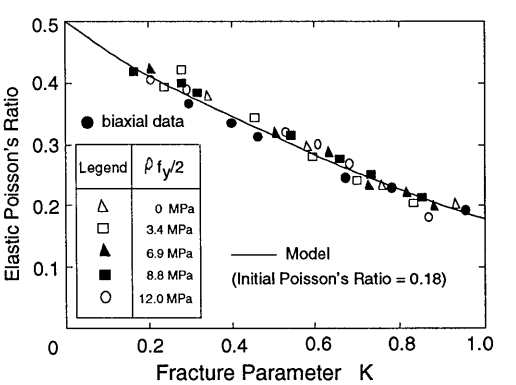

Fig.13 Elastic Poisson's Ratio of Damaged Concrete

$$M_{ijkl} = 2G_o K\delta_{ik}\delta_{jl} + \frac{1}{3}[(3K_o - 2G_o K)\delta_{ij}$$

$$+ 2G_o e_{eij} U_f \left(\frac{\partial K}{\partial F}\right)\left\{\left(\frac{\partial F}{\partial I_{1e}}\right) - \frac{2}{3}\left(\frac{J_{2e}}{J_{3e}}\right)^2\left(\frac{\partial F}{\partial J_{3e}}\right)\right\}]\delta_{kl}$$

$$+ 2G_o e_{eij} U_f \left(\frac{\partial K}{\partial F}\right)\left[\left(\frac{\partial F}{\partial J_{2e}}\right)\frac{e_{ekl}}{2J_{2e}} + \left(\frac{\partial F}{\partial J_{3e}}\right)\frac{e_{ekm}e_{elm}}{3J_{3e}^2}\right] \tag{14b}$$

$U_f = 1$, when $F=F_{max}$ and $dF > 0$
$U_f = 0$, otherwise

The propriety of the tensorial expression can be examined with regard to the elastic Poisson's ratio of the fracture continuum. If the fracture can be definitely associated with the deviatoric one in terms of the volumetric elasticity, the elastic Poisson's ratio remains constant and independent of the damage [9]. The elastic Poisson's ratio can derive from the compliance of the stress and elastic strain relation. The total elastic strain is described in turn by the hydrostatic and deviator stress tensors as,

$$\varepsilon_{eij} = I_{1e}\delta_{ij} + e_{eij} = \left(\frac{I_1}{3K_o}\right)\delta_{ij} + \frac{s_{ij}}{(2G_o K)} = C_{ijkl}\sigma_{kl} \tag{15a}$$

where,

$$C_{ijkl} = \frac{1}{(2G_o K)}\delta_{ik}\delta_{jl} + \left\{\frac{1}{9K_o} - \frac{1}{2G_o K}\right\}\delta_{ij}\delta_{kl} \tag{15b}$$

The apparent elastic Poisson's ratio of the damaged concrete is equal to $-C_{xxyy}/C_{xxxx}$ as a function of the fracture parameter. Here, the fracture parameter remains unchanged. From Eq.(15), we have,

$$\nu_e = \frac{1 + \nu_o - K(1 - 2\nu_o)}{2(1 + \nu_o) + K(1 - 2\nu_o)} \tag{16}$$

The elastic Poisson's ratio obtained from the unloading or reloading path is shown in Fig.13; this comes from triaxial and biaxial loading tests. The precision of Eq.(16) seems reasonable. The shear fracture isotropy in Eq.(12) is practically applicable. The theoretical maximum value of ν_e is 0.5, whatever the initial Poisson's ratio. This prediction was verified also on biaxial stress paths [1].

2.7 Concluding Remarks

The nonlinearities appearing in the deformational behavior of concrete under triaxial stresses was separated into plasticity and elasticity. Continuum fracturing was defined as the reduced stiffness and associated loss of volume which can store the elastic strain energy. The elasticity of fractured concrete was investigated in terms of the isotropic (volumetric) and deviator (shear) components as follows.

(1) Within the range where hydrostatic stress is less than 60% of the uniaxial compressive strength, the capacity for volumetric elastic strain energy does not deteriorate no matter how mechanical defects such as micro-cracks are induced.

(2) Continuum fracturing appears in terms of the elastic strain energy of the deviatoric (shear) mode. The elastic shear stiffness irreversibly decreases when defects accumulate. The hydrostatic component of stress was found to sensitively affect the rate of fracture when the elastic shear strain increases.

To predict the fracture parameter (the reduction in shear elasticity), the elastic strain invariants are adopted as representative of the internal stress intensity, and thus as determinants of microscopic fracturing. The tensorial expression of constitutive equation for elasticity of the fractured concrete was derived. The path-dependent Poisson's ratio in unloading and reloading was theoretically derived from the constitutive law and experimentally verified.

A fully formulated constitutive equation will be formed by combining the continuum fracturing model for the elastic component with the plasticity, which will be discussed in the next chapter.

3. PLASTICITY IN CONCRETE NONLINEARITY UNDER TRIAXIAL CONFINEMENT

3.1 General

Plasticity is a major factor in the nonlinearity of concrete along with continuum fracturing. This chapter aims at a constitutive law for the plasticity component of the overall deformation of damaged concrete under triaxial confinement.

Three-dimensional (3D) confinement is known to improve the ductility and strength of concrete. Within the framework of plasticity theory, the strength gain under 3D compressive stresses has been described by the plastic loading function [15]. The plastic hardening rule automatically implies a positive definite stiffness on the total stress-strain curve and remain constant along unloading path. However, softening along both the loading and unloading paths takes place when confinement is not very great, as in RC columns with lateral ties [10]. The concept of plasticity is not enough to cover the full nonlinearities of concrete [1]. The authors have adopted the elasto-plasticity and fracturing concepts as a generic constitutive law for damaged concrete [1].

The nonlinearities of concrete were separated into the continuum fracture discussed in the previous section, and the plasticity, which is the focus of this section, as illustrated in Fig.2. The target problem is to formulate the plasticity of the damaged continuum. Unlike the stress-based plastic function and hardening rule [15], the elastic strain is newly adopted to specify plasticity since elasticity is regarded as an indicator of internal stress intensity for a damage continuum with micro defects [1] (see Section 2.5). The key to this section is to extract the "*effect of confinement*" on the plasticity of damaged concrete with stress-induced defects within the framework of elasto-plastic and fracture scheme shown in Fig.2.

3.2 Internal Stress Intensity for Damaged Continuum

As shown in Fig.1, concrete can be idealized as a bundle of infinitesimal elasto-plastic elements. Continuum fracturing is represented as a loss of elastic strain energy. Since the total stress is the resultant of the component stress of the damaged system, the total stress does not represent the internal stress intensity applied to component which behaves as an elasto-plastic body.

The elastic strain implies an internal stress applied to the active and non-damaged elasto-plastic component. The authors take the elastic strain invariants I_{1e} and J_{2e} as indicators of the internal stress intensity for the damage continuum as Eq.(3a) and Eq.(3b). The value of I_{1e} indicates the hydrostatic internal stress intensity and J_{2e}, the deviatoric (shear) intensity. The continuum fracture theory relates the above mentioned indicators to the total applied stresses. The problem to be solved here is how to relate the elasticity to the plasticity of concrete under generic 3D stresses.

3.3 Shear Plasticity

Shear plasticity - denoted by the elastic deviator tensors - means the distorted residual deformation of the concrete. Even if the updated plastic strain is the same at a specific time, the shear plastic work consumed by the active component must differ if different paths are adopted, i.e., the closed-loop plasticity path gives rise to a plastic energy consumption as shown in Fig.14. This implies that the indicator of plasticity has to be defined path-dependently, too. First, let us evaluate the specific shear plastic work per unit volume of active non-damaged components, as shown in Fig.1. As mentioned, the elastic strain represents the internal stress intensity on the elasto-plastic component. Thus, we have,

$$W_{ps} = \int dW_{ps} \tag{17a}$$

$$dW_{ps} = 2G_o e_{eij} de_{pij} \tag{17b}$$

where, $d\,e_{pij} = d\,\varepsilon_{pij} - d\,(\varepsilon_{pkk}/3)\,\delta_{ij}$ and G_o is shear elastic stiffness. In Eq.(17), e_{pij} and W_{ps} are the plastic deviator tensors and the specific shear plastic work defined on the basis of effective volume regarding the non-damaged elasto-plastic component as shown in Fig.1, respectively.

According to Eq.(17), a different deformation path gives rise to a different net plastic work. Extending the two-dimensional equivalent plastic strain [1] to three-dimensional, the authors here propose the following plastic deviator invariant based on the path-dependent specific plastic work expressed:

$$J_{2p} = \int dJ_{2p} \tag{18a}$$

$$dJ_{2p} \equiv \frac{dW_{ps}}{2(2G_o J_{2e})} = \frac{e_{eij} de_{pij}}{2J_{2e}} = \frac{\partial J_{2e}}{\partial \varepsilon_{eij}} d\varepsilon_{pij} \tag{18b}$$

The increment in plastic deviator invariant J_{2p} is defined as proportional to the increment in specific shear plastic work defined for the non-damaged volume and normalized by the internal deviator stress intensity denoted by $2\,G_o\,J_{2e}$. Then, J_{2p} is mechanically path dependent and plastic work oriented. In cyclic loading tests using steel-ring-confined cylinders, J_{2p} was calculated by conducting the path integration shown in Fig.15.

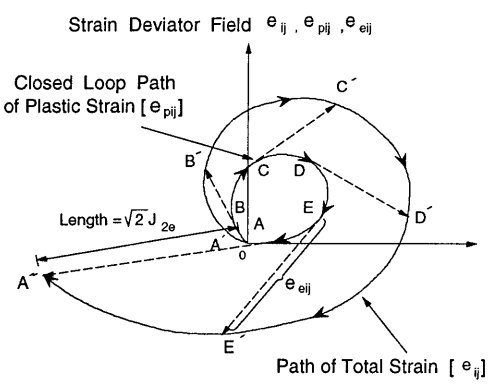

Fig.14 Plastic Work in Closed Loop

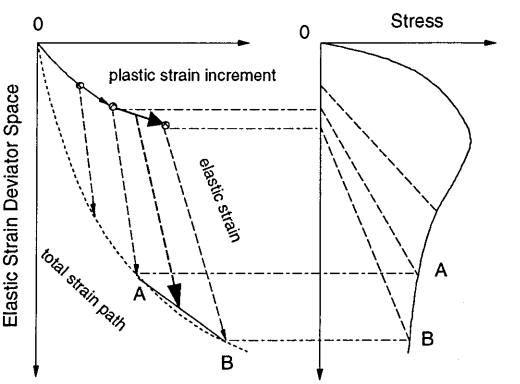

Fig.15 Path Integral of Plastic Indicator in Shear Mode

The relationship between J_{2p} and J_{2e} which is in fact equal to J_{2emax}, i.e., the maximum of J_{2e} throughout the loading history, is shown in Fig.16, where ρ and f_y are the volume ratio of steel casing to concrete and the yield strength (see Fig.5). The isotropic lateral stress when the steel reaches the yield point is equal to $\rho f_y/2$, and ranges from 0 (uniaxial) to 12 MPa experimentally. As an extreme case, the data for isotropic biaxial compression tests is included in Fig.16. Even though the level of confinement is different, the J_{2p} - J_{2e} relation remains unchanged. As far as the evolution of the shear plasticity specified by Eq.(18) is concerned, no effect of confinement is seen. The authors propose that the deviatoric component of plasticity is a function of internal shear intensity (J_{2e}) only. The empirical polynomial equation which fits the data shown in Fig.16 was found to be

$$J_{2p} = H(J_{2e}) = \frac{9}{10}\varepsilon_o\left(\frac{J_{2e}}{\varepsilon_o}\right)^3 \tag{19a}$$

$$\frac{dJ_{2p}}{dJ_{2e}} = 0 \qquad \text{when} \qquad J_{2e} = 0 \tag{19b}$$

$$\left(\frac{dJ_{2p}}{dJ_{2e}}\right)^{-1} = 0 \qquad \text{when} \qquad J_{2p} = \infty$$

where, ε_o which is defined in Eq.(7b) is the material constant which makes Eq.(19a) applicable to normal aggregate concrete with a strength from 15MPa to 50 MPa [5,10,18]. Notations E_o and $\nu_o$mean the initial elasticity coefficient and Poisson's ratio, respectively. Equation (19a) was designed so that the conditions at two extreme cases satisfy certain conditions.

The first condition specifies no plastic progress at the very beginning of loading, and the second mathematically specifies perfect plasticity when the deformation is infinitely large. As shown in Fig.16, the curve fitting seems satisfactory within the range of the test data.

A similar mechanism is observed in the stress transfer behavior along a crack in the concrete. Li et al. [14] reported that the total shear slip or elastic shear slip versus plastic shear slip relation is not affected by the crack confinement stress when the crack width remains unchanged. In both cases, of course, the shear stress and shear plasticity relations appear to be influenced by the confinement level. But when we select elasticity as an indicator of plasticity arising in the damage continuum, we can easily treat the plasticity as similar to that of Von-Mises based materials [15].

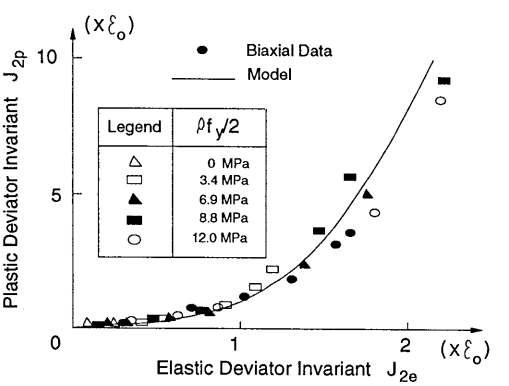

Fig.16 Plastic Evolution of Damaged Continuum in Shear Mode

3.4 Volumetric Plasticity

(1) Dilatancy

The plastic deviator invariant was proposed as the equivalent plasticity in shear in Section 3.3 based on the specific shear plastic work consumed by the non-damaged volume of concrete. A similar approach will be adopted in terms of the volumetric plasticity. The net plastic work in the volumetric mode is

$$dW_{pv} = 3K_o I_{1e} d\left(\frac{\varepsilon_{pkk}}{3}\right) \tag{20}$$

where, K_o is the volumetric elastic stiffness equal to $E_o/3(1-2\nu_o)$. Similarly to the definition of J_{2p}, we define the volumetric plastic invariant I_{1p} as,

$$dI_{1p} \equiv \frac{dW_{pv}}{3K_o I_{1e}} = d\left(\frac{\varepsilon_{pkk}}{3}\right) \tag{21}$$

Then, we have,

$$I_{1p} = \int dI_{1p} = \frac{1}{3}\varepsilon_{pkk} \tag{22}$$

The volumetric plastic invariant is a plastic work based definition too, but unlike the plastic deviator invariant, the integral in Eq.(22) results in path-independency. Figure 17 shows experimentally obtained data for the I_{1p} versus J_{2p} relations in the case of steel-encased concrete cylinders with different levels of steel confinement. These test data were drawn also from cyclic cylinder tests with lateral confinement by steel rings as shown in Fig.5. The volumetric plasticity appears to be associated with the deviator component in plasticity denoted by J_{2p}, and unlike the discussion in the previous chapter, different confinement gives rise to a different path on the J_{2p} versus I_{1p} plane. Hereafter, the change in volumetric plasticity associated with the shear plasticity is defined as "*dilatancy*" in the same manner as in continuum mechanics. According to Fig.17, we can conclude that an effect of confinement on the dilatancy definitely exists. It may be allowable to define the dilatancy derivative D as,

$$D \equiv \frac{\partial I_{1p}}{\partial J_{2p}} \tag{23}$$

The value of D is the gradient of the I_{1p} - J_{2p} relation as shown in Fig.17. In all cases of confinement, the value of D is negative when the shear plasticity is smaller. Similar behavior is reported in investigations of sand. With lower plasticity, the rearrangement and consolidation of sand particles are thought to take place [16], which causes negative dilatancy. After that, the dilatancy derivative turns positive going from volumetric contraction to expansion. Figure 18 shows the dilatancy derivative with the isotropic elasticity I_{1e} as an indicator of confinement and the fracture parameter K [1] as representative of the damage of elasticity. The experimental values of D were obtained by taking the mean gradient between two adjacent plastic invariants. The corresponding fracture parameter and the volumetric invariant are represented by the mean values of measured data between two adjacent plasticities in cyclic loading. The information on plasticity, elasticity, and fracturing was obtained at each stress state by conducting cyclic compression loading on steel-confined concrete.

The results seem reasonable. The higher the confinement, the smaller the dilatancy. The more heavily the concrete is damaged, the more dilatancy is observed. It is understood from the results that shear-induced

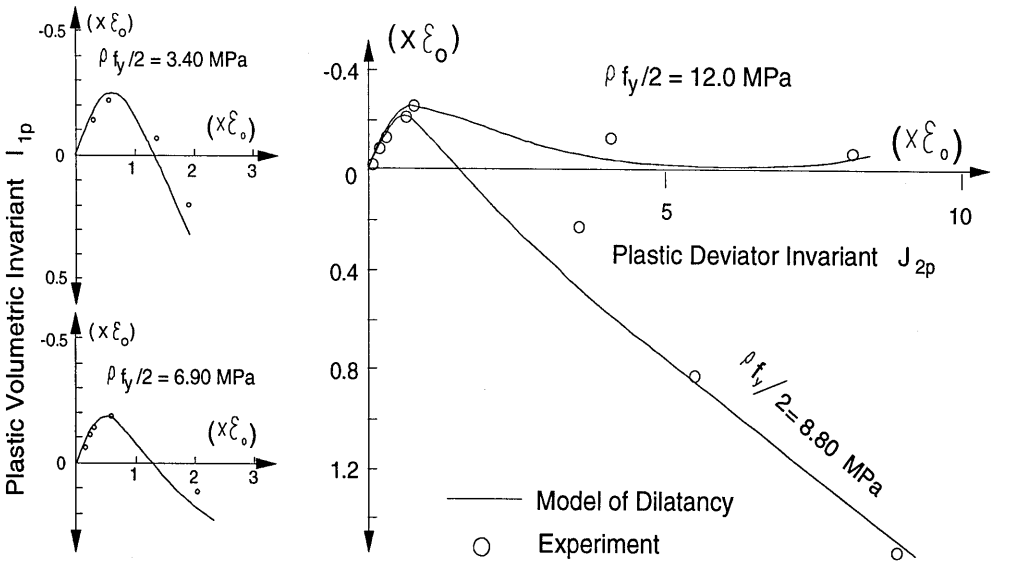

Fig.17 Volumetric Plasticity Associated with Shear Plasticity : $\varepsilon_o = 0.0025$, $f_c' = 29$MPa

plastic expansion is proportional to confinement and updated damage condition of the fracture continuum. Based on the data shown in Fig.18, the following empirical formulas are here proposed for normal aggregate concrete with a uniaxial compressive strength of 15-50 MPa:

$$D = D_o \qquad K \geq 0.5$$

$$= D_o(2K)^2 + D_1(1-4K^2) \geq D_o \qquad K < 0.5$$

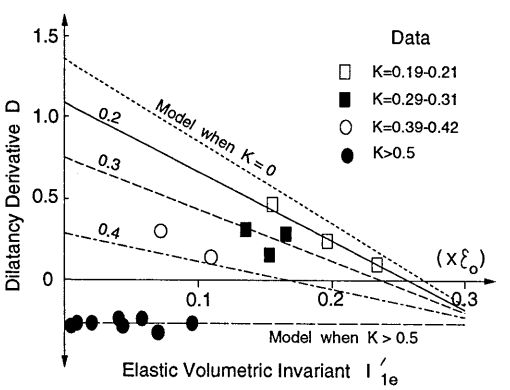

Fig.18a Effect of Confinement on Dilatancy

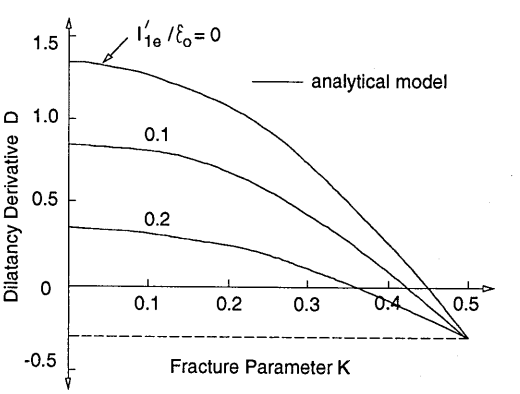

Fig.18b Effect of Fracture Parameter on Dilatancy

where,

$$D_1 = \frac{\sqrt{2}I_{1e} + 0.38\varepsilon_o}{0.28\varepsilon_o} \quad , \quad D_o = -\frac{1-2\nu_o}{\sqrt{3}(1+\nu_o)} \tag{24}$$

$$K = \frac{J_2}{2G_o J_{2e}} \quad , \quad J_2 = \sqrt{\frac{1}{2} s_{ij} \cdot s_{ij}}$$

The initial value of derivative D_o is set so that the plastic Poisson's ratio coincides with the initial elastic Poisson's ratio when the level of fracturing is lower [1]. The plastic Poisson's ratio and the derivative can be theoretically related by completing the flow rule. Concerning the mathematical conditions on the initial derivative D_o, refer to coming Section 3.7 and Eq.(30) in detail. The value of D_1 in Eq.(24) is the hypothetical derivative corresponding to the complete fracture continuum in which K is zero. In this case, the predictive model by Eq.(24) becomes borderline in Fig.18a (small-dotted line), and the constitutive model of dilatancy is thought to work for an assembly of fractured pieces of concrete with plenty of crack surfaces. This extreme case can hardly be realized in experiment. This value was fixed through extrapolation of existing data as shown in Fig.18a and Fig.18b.

The opening of discrete cracks in concrete under normal compression [14] is comparable with the effect of confinement on dilatancy which is of concern here. Crack opening associated with shear slip is reported to be affected by the level of normal compression, but no effect of confinement is seen on the plastic shear slip vs. elastic slip relation for a single discrete crack in concrete. There are common features shared by the crack shear and 3D plasticity of concrete. Therefore, the value of $D_1(I_{1e} = 0)$ - which cannot be identified by experiment - was chosen so that it coincides with the dilatancy factor of a single concrete crack (rate of crack opening / rate of shear slip along the crack) when the normal compression is equal to zero [19].

It can be presumed that the macroscopic plasticity of the 3D continuum of concrete derives from an assembly of dispersed defects which behave similarly to discrete concrete cracks if the damage is lesser. The dilatancy of the fracture continuum was interpolated between D_o and D_1 according to the fracture parameter.

(2) Consolidation

Growth of the volumetric plasticity is enhanced not only by the dilatancy, which is assumed to be the opening of defects under shear, but also by volumetric compression. This mechanism might be called plastic consolidation or compaction, and it is not related to the micro defects induced. Kotsovos [17] reported volumetric stress strain tests without any shear mode nor a dilatancy mechanism. The volumetric plasticity can be recognized under volumetric stress action only. However, compared with volumetric expansion due to dilatancy resulting from internal damage, the compaction seems to be negligible when we discuss the 3D deformability of concrete under confinement less than 40 MPa in terms of hydrostatic stress. In this model, for simplicity, the authors neglected the volumetric compaction due to isotropic compression in plasticity.

3.5 Flow Rule

The above discussion is valid for the relationship between invariants. To finalize the tensorial expression of plasticity, the flow rule - which specifies the direction of the plasticity - is indispensable. Using the hollow cylinder specimens subjected to combined compression-torsion, Li et al. [2] reported coincidence between the principal direction of plastic increment with that of the updated stresses. This means that the plastic shear increment does not develop on coordinates parallel to the principal axis of elastic strains. The simplest expression of the flow rule which satisfies this conditions is,

$$de_{pij} = e_{eij} dg \tag{25}$$

where, dg is the proportional coefficient.

On a coordinate system based on the principal elastic strain, the shear components e_{eij} $(i \neq j)$ become practically zero. Therefore, no progress in shear plastic increment $d\,e_{pij}$ (i≠j) is automatically satisfied [2]. The above flow rule stated in terms of the deviatoric component, holds exactly when isotropic confinements such as those in cylinder tests and biaxial compression tests are realized.

Figure 19 shows the π-plane on the principal elastic strain field. Since a shear plasticity is enhanced by the elastic deviator invariant alone, the envelope in which J_{2e} is constant becomes a circle on the plane. According to the shear flow of plasticity given by Eq.(25), the incremental plastic deviator vector $<d\,e_{pij}>$ is parallel to the normal vector in the envelope with constant J_{2e}.

For isotropic confinement where the two principal stresses are the same (A and B in Fig.19), we can expect the same plastic increment in the confinement direction. Here, the direction of plastic incremental vector projected on the π-plane coincides with the normal vector in the envelope formed on the elastic strain field as denoted by Eq.(25). The normality of plasticity on the elastic plane seems reasonable as a first assumption. However, if general cases are considered rather than isotropic confinement, the applicability of the flow rule must be verified at the structural member level again.

3.6 Tensorial Expression of Plastic Constitutive Law

By combining the plastic incremental deviator tensor expressed by Eq.(25) and the corresponding invariant in shear defined by Eq.(18), we obtain a plastic proportional coefficient in terms of the increment in the invariant as follows.

$$dJ_{2p} = \frac{e_{eij} de_{pij}}{2J_{2e}} = \frac{e_{eij} e_{eij}}{2J_{2e}} dg \tag{26}$$

$$= J_{2e} dg$$

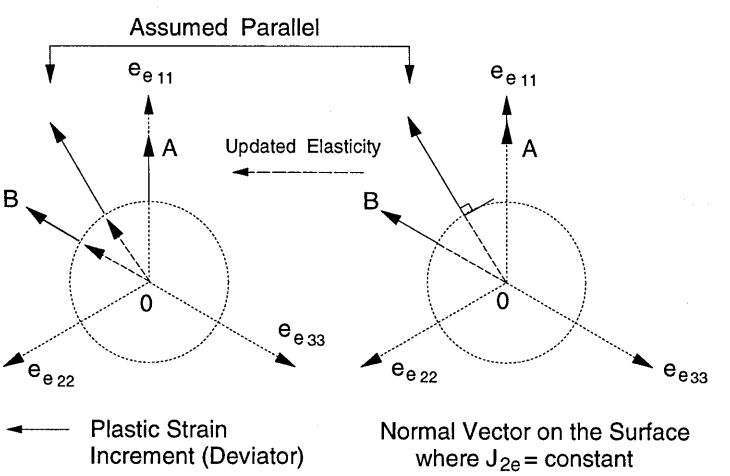

Fig.19 Plastic Incremental Direction and Normal Vector on Deviator Surface

Then, we have,

$$\begin{aligned} d\varepsilon_{pij} &= de_{pij} + \delta_{ij} dI_{1p} \\ &= e_{eij} \frac{dJ_{2p}}{J_{2e}} + \delta_{ij} D dJ_{2p} \\ &= \left\{ \frac{e_{eij}}{J_{2e}} + \delta_{ij} D(I_{1e}, K) \right\} \left(\frac{dH}{dJ_{2e}} \right) U_p dJ_{2e} \end{aligned} \tag{27}$$

where,

$U_p = 1$, when $d(J_{2e}) > 0$ and $J_{2e} = J_{2emax}$
$U_p = 0$, otherwise

The total differentiation of J_{2e} can be described in terms of the increment in elastic strain as,

$$\begin{aligned} dJ_{2e} &= \frac{e_{ekl} de_{ekl}}{2J_{2e}} = \frac{e_{ekl}}{2J_{2e}} d\left(\varepsilon_{ekl} - \frac{1}{3} \delta_{kl} \varepsilon_{emm} \right) \\ &= \frac{e_{ekl} d\varepsilon_{ekl}}{2J_{2e}} \end{aligned} \tag{28}$$

By substituting Eq.(28) into Eq.(27), we obtain the plastic constitutive equation for the damage continuum in terms of the elastic strain increment, as follows.

$$d\varepsilon_{pij} = L_{ijkl} d\varepsilon_{ekl} \tag{29a}$$

$$L_{ijkl} = \left(\frac{e_{eij}}{J_{2e}} + D\delta_{ij} \right) \left(\frac{dH}{dJ_{2e}} \right) \frac{U_p e_{ekl}}{2J_{2e}} \tag{29b}$$

3.7 Verification

To verify the plasticity constitutive law described above, we must solve the plasticity constitutive equation and the fracture equation simultaneously, because the fracture parameter K is involved in the plasticity model. The plastic constitutive law for damaged concrete is coupled to the fracture elasticity. We can expect better applicability to three-dimensionally confined concrete because the material parameters were specified so that they match the experimental data. Thus, verification must be conducted based on data not directly utilized in setting up the model. Here, the plastic Poisson's ratio can be checked under a simple uniaxial stress state. The plastic biaxial strain under uniaxial stress has been reported by Maekawa and Okamura [1]. First, let us consider the uniaxial stress in the 1 (x) direction. From Eq.(29), the plastic Poisson's ratio defined as ν_p becomes

$$\begin{aligned} \nu_p &= -\frac{d\varepsilon_{p22}}{d\varepsilon_{p11}} = -\frac{e_{e22} + DJ_{2e}}{e_{e11} + DJ_{2e}} \\ &= -\frac{s_{22} + DJ_2}{s_{11} + DJ_2} = \frac{1 + \sqrt{3}D}{2 - \sqrt{3}D} \end{aligned} \tag{30}$$

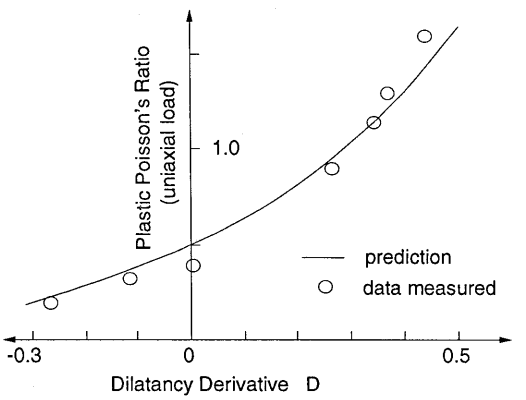

Fig.20 Plastic Poisson's Ratio under Uniaxial Stress States

where,

$$D = D(K, I_{1e}) = D\left(K, \frac{\sigma_{11}}{9K_o}\right)$$

Figure 20 shows the relationship between plastic Poisson's ratio and the dilatancy derivative. With an increase in dilatancy, the plastic Poisson's ratio increases. Since the dilatancy derivative is a function of the total stress and the fracture parameter, which is uniquely governed by the uniaxial stress, the plastic Poisson's ratio is controlled by the stress under uniaxial compression as discussed by Maekawa, et al [1]. In the experiment, the values of ν_p, K, and σ_{11} were measured. The relationship between these three measured values is drawn up in terms of the plastic Poisson's ratio and the dilatancy derivative in Fig.20. The analytical model looks reasonable. When we solve the plasticity and continuum fracture equations simultaneously, the fracture parameter which is needed to compute Eq.(30) is self consistent with the plasticity. The authors will report on combined plasticity and fracturing in the next chapter and again verify the full constitutive equation with triaxial loading data.

In the next step, let us check the dilatancy model under triaxial compression. The analytically computed paths on the $<I_{1p}, J_{2p}>$ plane are shown in Fig.17. In this computation, the stress and corresponding fracture parameter are needed to conduct the integral denoted by Eq.(24). We can use the constitutive law of continuum fracturing to obtain the control parameters of Eq.(24). But, here the authors used the experimentally obtained stress value to evaluate I_{1e} and K purely for verifying the dilatancy model. In fact, the path integration was carried out numerically with respect to I_{1p} in using Eq.(23) and Eq.(24). The coincidence of the analysis with the experiments seems acceptable. Combination of this with the continuum fracture model will be discussed in the next section.

3.8 Concluding Remarks

From the overall nonlinear behavior of concrete under triaxial stresses, the plasticity was abstracted. The main feature of the plasticity constitutive law of concrete is the plasticity of the mechanically damaged continuum with stress induced defects. The elastic strain component was assigned as the indicator of internal stress intensity in the damage continuum based on the elasto-plasticity and fracturing concepts. The total stress was not considered in formulating the model. In this paper, three-dimensional confinement of the fractured concrete was clearly evaluated as the first invariant of elasticity. The following effects of confinement on the plasticity of concrete were manifested.

(1) The evolution of deviatoric plasticity was uniquely determined by the deviatoric elastic invariant. This means no effect of confinement was found in the development of deviatoric plasticity. However, if the total stresses were adopted as the main parameter, we would have a confinement-dependent relation for plasticity and stress as reported in the past. The elasticity was proven to be appropriate as an expression of internal stress intensity.

(2) The dilatancy, which is the volumetric plasticity associated with the shear plasticity, was much affected by the confinement and the updated degree of concrete damage. A higher confinement was proven to reduce the dilatancy. Greater continuum fracturing makes the dilatancy more significant. These characteristics are macroscopic ones. It was found that a similarity with continuum plasticity exists in the case of discrete crack plasticity in concrete.

The tensorial expression of plasticity was derived by combining the conclusions mentioned above and the simple flow rule, which specifies the direction of increments in plastic strain. In this study, elastic strain-based normality was newly introduced since the elastic strain has a direct proportional relationship with the internal stress intensity. The plasticity loading function was not associated with the failure envelope, in contrast with the classical normality rule of plasticity, because the failure envelope must be associated with both plastic hardening and continuum fracturing. The authors defined the plastic potential in terms of the constant elastic deviator invariant for simplicity.

The newly proposed flow rule based on elastic strain field and other material-oriented models were indirectly verified by checking the theoretical and experimental Poisson's ratios of incremental plasticity. Since the plastic model for a damage continuum includes a fracture parameter to indicate damage conditions, it is essential to again verify the plasticity model in combination with the model of continuum fracturing. This will be discussed in the next chapter.

4. TRIAXIAL ELASTO-PLASTIC AND FRACTURE MODEL FOR CONCRETE

4.1 General

Design-oriented constitutive models for fiber stress in flexural members confined by lateral reinforcement can be said to be spatially averaged models applicable to particular members. The local stress and strain induced by the three-dimensional (3D) arrangement of lateral steel has not been directly considered yet; rather, the mean stress versus mean strain relation has been the main concern of practitioners [27].

Accordingly, the spatially averaged stresses have included the spacing, shapes of lateral ties, the yield strength of steel, and other factors [28]. The averaged model can be approximated through laterally reinforced column tests subjected to uniform axial compression, but the mean fiber stress under the eccentric loads cannot be obtained by this method. This spatially averaged constitutive model is convenient for structural member design but at the same time its applicability is narrow.

The other approach is to take into account the 3D local stress as it is, whatever geometrical condition of lateral confinement is specified. To the authors' knowledge, Inoue et al. [20] were the first to apply finite element analysis to steel-confined columns. This approach was very strategic despite computational difficulties, because of its generality and versatility. The 3D computational evaluation of the strength and ductility of members relies on the constitutive law for concrete under triaxial stresses. To realize this generic method, the authors have proposed continuum 3D fracturing and plasticity constitutive laws for the damage continuum of concrete in Chapter 2 and Chapter 3. In this chapter, the aim is to finalize a general 3D constitutive equation by combining the elasticity, fracturing and plasticity of concrete, which is regarded as the damage continuum, in the framework of elasto-plastic and fracture concept as illustrated in Fig.2.

This chapter will also serve to verify the complete constitutive equation based on cyclic loading tests of concrete under triaxial stresses. Since the application of this model is oriented toward laterally confined RC columns, the accuracy of the model will be verified mainly under comparatively low confinement conditions.

4.2 Full Constitutive Matrix

Concrete can be regarded as a damage continuum with plasticity [1] as mentioned before and shown in Fig.1. The total stress is idealized to be the sum of the internal stresses developing in non-damaged constituent elements. It can be understood from Fig.1 that the elastic strain is directly proportional to the internal stress applied to active non-damaged elasto-plastic elements. Then, the elastic strain is taken to represent the internal stress intensity, which governs the plasticity and fracturing of the continuum with defects [1].

Under triaxial stress states, the following brief summaries concerning the fracturing and plasticity constitutive laws can be made in terms of volumetric and deviatoric components.

(1) *Hydrostatic Fracturing*: The capacity to store volumetric elastic strain energy is not damaged regardless of the magnitude of the defects induced in the concrete and of the confinement denoted by I_{1e}. This law is represented by Eq.(4).

(2) *Shear Fracturing*: The absorption of shear elastic strain energy deteriorates according to the state of load-induced fracturing. The growth of continuum damage, denoted by the fracture parameter K, is boosted by internal shear stress intensity, represented by J_{2e} and J_{3e}, but suppressed by the confinement, denoted by I_{1e}. This law is formulated as Eq.(5) and the evolution rule by Eq.(10).

(3) *Shear Plasticity* : The plastic deviator in shear is enhanced by the internal shear stress intensity expressed by J_{2e} but not influenced by the magnitude of confinement. This plastic constitutive law is expressed by Eq.(18) and its evolution law is given by Eq.(19).

(4) *Volumetric Plasticity* : The volumetric plastic strain associated with the shear plasticity is significantly affected by the magnitude of the confinement indicated by I_{1e}. This nonlinearity is named the shear dilatancy indicated by the dilatancy derivative defined by Eq.(23) and regulated by Eq.(24).

The "*effects of confinement*", which have been of great interest, are classified into continuum fracturing and plasticity in terms of volumetric and deviatoric aspects, respectively. The above four constitutive laws are the core of the continuum fracturing and plasticity constitutive laws.

The main objective of this chapter is to combine the fracturing elasticity and plasticity of the damaged concrete. In both cases, the control parameters are specified as an elastic strain which represents the internal stress intensity as shown in Fig.1. There have been other attempts to combine the plasticity and continuum damage [25,26], where the damage and plasticity were formulated with respect to the total stress and strain. Since the internal stress intensity, as the driving action behind damage and plasticity, is not explicitly adopted, the physical meaning of plastic and fracture surfaces (functions) used becomes vague. On the other hand, regarding elasticity as directly proportional to internal stress intensity is the main feature of this model. For structural analysis, the total strain has to explicitly appear in the final constitutive equation. According to the deformational compatibility, we have,

$$d\varepsilon_{ij} = d\varepsilon_{eij} + d\varepsilon_{pij} \tag{31}$$

A combination of Eq.(14), Eq.(29) and Eq.(31) yields the full incremental constitutive equation. The matrix form of the combined elasto-plastic and fracture model is ultimately brought to completion as,

$$d\{\sigma\} = [M]\,([I] + [L])^{-1} d\{\varepsilon\} \tag{32}$$

where [M] and [L] express the fracture and plasticity matrix of the fourth order tensors D_{ijkl} and M_{ijkl} in Eq.(14) and Eq.(29). It may be difficult to derive the full fourth-order tensorial expression for the total stress-strain incremental relation in Eq.(32), because a non-symmetry arises in matrix [L] due to the presence of dilatancy.

4.3 Material Constants and Functions

(1) Concrete

From 2D and 3D cyclic loading data, material functions are proposed for concrete with normal aggregate and strength ranging from 15MPa to 50MPa.

The fracture function K in Eq.(10) represents the degradation of shear elastic strain energy for concrete including defects. The plastic hardening function H in Eq.(19) indicates plastic hardening of the internal plastic element in the damaged concrete (see Fig.2). The derivative D in Eq.(24) represents the plastic dilatancy induced by shear plastic dislocation along internal defects.

(2) Steel

The 3D constitutive law for steel must be incorporated into the one for concrete when concrete columns are laterally confined by steel in the analysis. This section will prove a general elasto-plastic and fracture model for concrete covering the elasto-plastic behavior of steel by a plasticity theory incorporating the Von-Mises yield function. Let the fracture parameter K remain constant (=1). This means that the material concerned does not undergo any fracturing (see Fig.2) with regard to the elastic strain energy. Further, the structural steel has no plastic dilatancy. The dilatancy derivative D has to be set at null. By assuming unity and null for these two functions, we have,

$$de_{pij} = e_{eij}dg = \frac{s_{ij}}{2G_o}dg = s_{ij}dg' \tag{33}$$

$$dI_{1p} = 0 \tag{34}$$

where, dg and dg' are proportional coefficients. Since fracturing is ignored, the total stress itself indicates the intensity of the internal stresses directly. The incremental form of plasticity is converted in terms of the stress tensors, and Eq.(33) and Eq.(34) then produce,

$$d\varepsilon_{pij} = de_{pij} + \delta_{ij}dI_{1p} = s_{ij}dg' \tag{35}$$

Differentiation of the second invariant of stress J_2 with respect to the total stress is proportional to the stress deviator. Then, we have another expression of Eq.(35) with the total stress tensors as,

$$d\varepsilon_{pij} = \left(\frac{\partial J_2}{\partial \sigma_{ij}}\right)dg'' \tag{36}$$

The non-fracture and non-dilatancy assumptions are eventually equivalent to Eq.(36), which is the same as the Prandtl-Reuss flow rule associated precisely with the Von-Mises plastic yield function applicable to structural steel. It can be concluded that the flow rule for steel in the theory of plasticity is a particular case of the proposed elasto-plastic and fracture model. The proportional coefficient dg'' specifies the magnitude of the plastic flow. When considering plasticity, the rate of plastic flow is determined by the plastic hardening rule [4]. In the proposed model, the plastic hardening function H takes on the role of actually specifying the proportional coefficient in Eq.(36). The proposed plastic hardening model in Eq.(19) is converted to,

$$\begin{aligned} dJ_{2p} &= \frac{dH}{dJ_{2e}}dJ_{2e} \\ &= \left\{\frac{dH}{dJ_{2e}}\left(\frac{J_2}{2G_o}\right)\right\}d\left(\frac{J_2}{2G_o}\right) \end{aligned} \tag{37}$$

According to the definition of the plastic second invariant by Eq.(18), we have another expression for the plastic rate provided that there is no dilatancy (D=0) and no fracturing (K=1) as follows.

$$dJ_{2p} = \frac{e_{eij} d\varepsilon_{pij}}{2J_{2e}}$$
$$= \frac{s_{ij}}{2J_2} d\varepsilon_{pij} \tag{38}$$
$$= \frac{\sigma_{ij}}{2J_2} d\varepsilon_{pij} - \frac{\sigma_{kk}}{2J_2} dI_{1p}$$

Substituting Eq.(38), where $d\,I_{1p}$ is equal to zero, into Eq.(37), we have,

$$\sigma_{ij} d\varepsilon_{pij} = \frac{J_2}{G_o}\left\{\frac{dH}{dJ_{2e}}\left(\frac{J_2}{2G_o}\right)\right\} dJ_2 \tag{39}$$
$$= H'(J_2) dJ_2 \qquad (= \text{plastic work})$$

The left side of Eq.(39) above represents the total plastic work. The plastic work is equated with the increment in plastic function represented by the second invariant of stress as indicated by Eq.(39). This expression is exactly the same as the work hardening formulation of plasticity [4]. The function H is originally expressed by the elastic strain. But, provided there is no fracturing, our function H is convertible to a hardening function H' which is controlled by the stress invariant used within the plasticity framework. The proposed constitutive laws are proven to cover conventional plasticity based on Von-Mises yield criterion.

4.4 Experimental Verification

It must be mentioned that the post-failure behavior (descending branch of the stress strain curve) is not covered by the model. This is because the continuum fracturing model used is applicable only when the defects are spatially distributed with little localization. When we come to expand applicability, the fracture indicator must be made size dependent, but at present, the formulation is not size dependent. Thus, in the following computation, the authors stop computation when the value of K reaches 0.35, which is thought to be the tentative limit of continuum fracturing.

(1) Confined cylinder

The axial stress-strain relationship for a concrete cylinder encased in steel is shown in Fig.21. The constitutive equation is solved with the following condition of steel confinement,

$$\sigma_{xx}' = \sigma_{yy}' = \rho\sigma_s(\varepsilon_{xx}) \tag{40}$$

where ρ is the volume ratio of encasing steel and σ_s is the hoop stress of steel associated with the lateral strain.

The dilatancy model incorporates lateral inelastic deformation, which in turn induces lateral stress, as well as the fracture model. Not only loading, but also the plastic residual strain coincide fairly well with the experimental data. The monotonic loading curve of axial stress under constant lateral pressure (σ_{xx}=σ_{yy}) is shown in Fig.22. The prediction is performed using step-by-step integration. The analytical results are close to the experimental data produced by Richart [21] and Kotsovos [22]. The precision of the prediction of the strength of hydro-pressured concrete relies primarily on the fracture function. The above stress condition will be of concern to structural analysts working on confined RC columns. The core concrete of circular and/or rectangular columns is thought to be in a triaxial stress state similar to the loading shown in Fig.22.

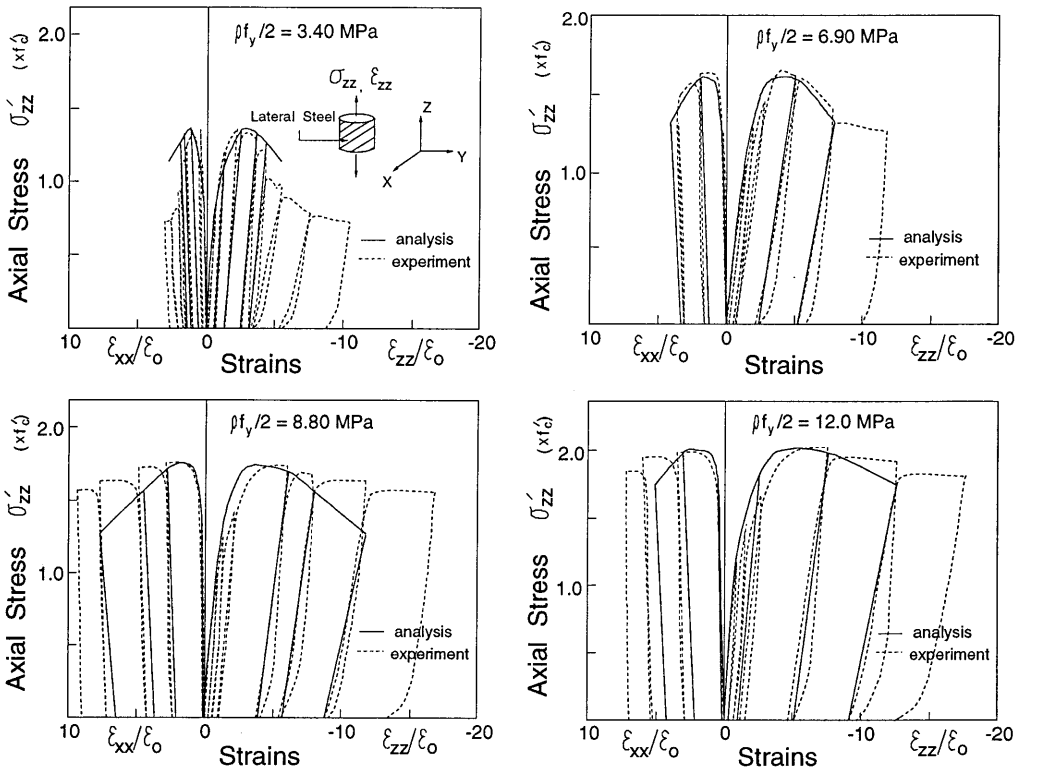

Fig.21 Stress-Strain Relation of Steel-Encased Cylinder : f_c'=29MPa, ε_o=0.0025

(2) Failure envelope

The failure envelope in stress space has been a principal target of triaxial loading tests undertaken in the past. This is because the obtained envelope is expected to be a plastic function within the framework of plasticity.

However, it is understood that a failure envelope which exhibits a set of stresses at failure is a material behavior to be computed based on both elasto-plasticity and fracturing model. Figure 23 shows the computed failure curve for different points on the equi-volumetric stress plane named π-plane [4]. The hydrostatic versus deviatoric failure curve is found to be affected by the effect of the third invariant on the continuum fracture. Failure is assumed when stress reaches peak stress, which presents the zero tangential stiffness. This means that the failure surface is characterized by a singular state where the fracturing softening upsets hardening owing to plasticity. The computed result is close to the experimental observations on both total stress planes. Both plastic hardening and fracture parameter are crucial to a determination of the failure conditions.

(3) Biaxial compression

The biaxial behavior is regarded as the general triaxial case viewed from a different angle. Access to the failure envelope was mainly gained through proportional loading paths in tests. The experiment by Kupfer et al. [24] and the prediction are shown in Fig.24. The biaxial failure surface is also a slice of the triaxial envelope. A minimal discrepancy is observed between the analysis and experimental data.

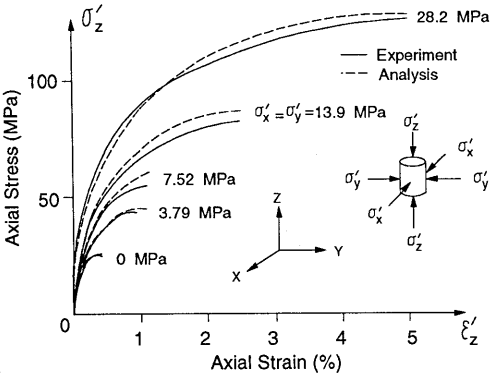

Fig.22a Stress-Strain Relationship for Hydraulically Confined Cylinder [21]

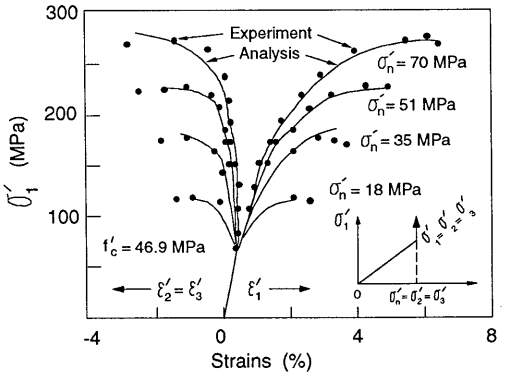

Fig.22b Stress-Strain Relationship for Hydraulically Confined Cylinder [22]

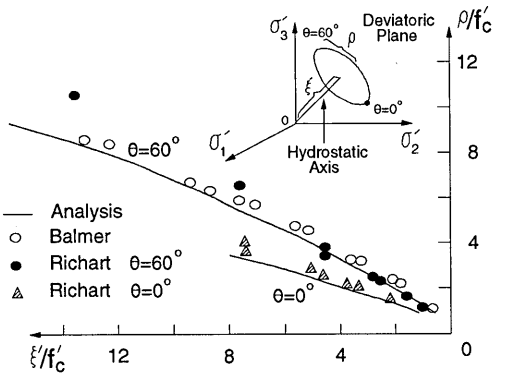

Fig.23 Failure Envelope in Stress Space [4,21,23]

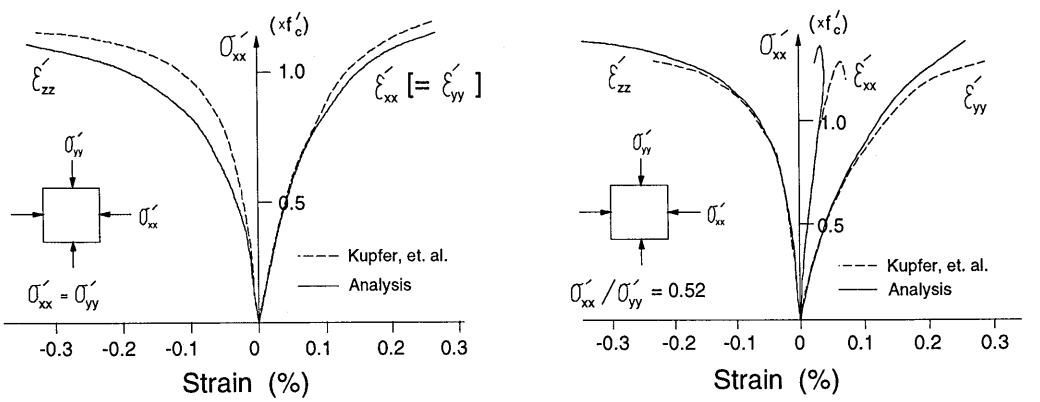

Fig.24a Isotropic and Anisotropic Biaxial Compression [24]

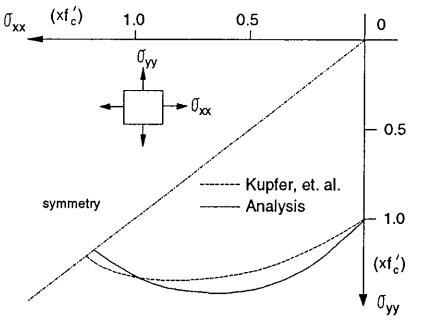

Fig.24b Biaxial Failure Envelop in Stress Space [24]

The strain paths on the biaxial plane under cyclic uniaxial stress are shown in Fig.25 [1]. When the stress exceeds approximately 90% of the strength, the strain path on loading becomes oriented with the direction equivalent to greater Poisson's ratio. A greater Poisson's ratio in unloading, which cannot be idealized within the frame of plasticity, is also found under uniaxial compression. These characteristics are associated with the model of combined dilatancy and fracturing. The uniaxial and biaxial stress state are also a concern in the structural analysis of laterally confined concrete columns with rectangular sections. The concrete located near lateral ties is subjected to stresses close to biaxial ones.

(4) Loading path

The unloading path from hydraulic compression was verified as shown in Fig.26 [17]. On this path, inelasticity (fracture and plasticity) and elastic recovery progress simultaneously. With this stress path, the models of elasticity, plasticity, and fracturing mutually correlate. The analytical result appears to match reality. In analysis, the initial elastic stiffness and Poisson's ratio were chosen so that the initial computed stiffness coincides with the experimental data.

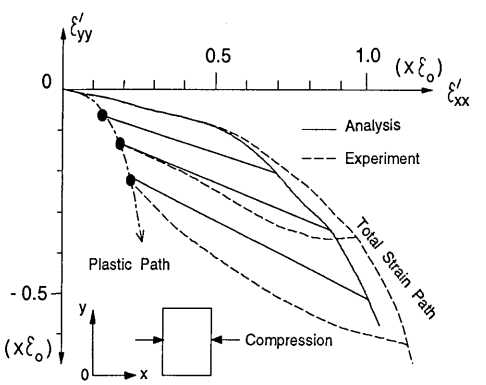

Fig.25 Biaxial Strain Path under Uniaxial Stress [1]

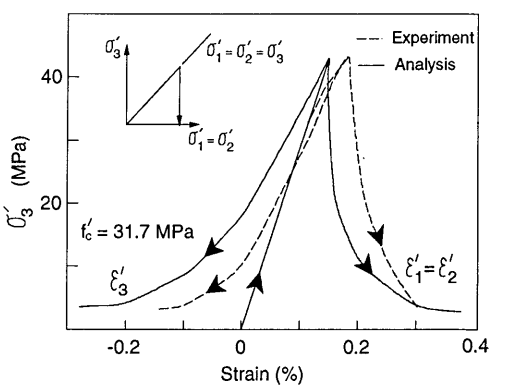

Fig.26 Unloading Path from Hydraulic Compression [17]

4.5 Concluding Remarks

The constitutive laws of continuum fracturing and plasticity for a damage continuum were combined under triaxial stress conditions, and the material functions and coefficients were proposed for normal aggregate concrete with a uniaxial compressive strength of 15-50 MPa. The full constitutive equation in terms of the stiffness matrix was formed with in the incremental form of the total stress and strain tensors. In this process, the elastic strain - which was utilized as the main parameter to determine plasticity and fracturing - was treated as the intermediate parameter.

Experimental verification was carried out for the stress-strain curve of steel-encased cylinders, computed failure envelopes and loading paths, and strain responses. The strength as specified by the loading path was not incorporated in the formulation but rather computed as a combination of plastic hardening and fracturing softening of elasticity. The comparison of computed triaxial strength with real strength thus became a check of plasticity as well as of fracturing model used. The versatility of the model proposed was examined. The formulated elasto-plastic and fracture model proved to cover the classical theory of plasticity linked to the Von-Mises yield function and the well-known associated flow rule by Prandtl-Reuss.

The development of this triaxial model was motivated by the needs for confined RC column analysis. The model finalized hereby will be utilized as a micro model in FEM for analyzing the confinement effects of lateral steel. The spacing of lateral hoops, the arrangement of intermediate ties, and the shape of cross section, which are thought to be influencing factors on the strength and ductility of RC columns, will be taken into account in structural analysis. Verification will be performed again at the structural member level.

5. CONCLUSIONS

Full constitutive laws of triaxial stress conditions based on an elasto-plastic and fracturing model are formulated. The complete formulation is based on the separate formulation of constitutive laws for fracturing and plasticity. Continuum fracturing is defined as a reduction in stiffness of the material related to its reduction in volume as it stores elastic strain energy. Plasticity is the residual deformation occuring in concrete when all the stresses are released. These two models are formulated based on their influence on the isotropic (volumetric) and deviator (shear) stresses inside the concrete. The effect of confinement on each of these factors is identified and can be summarized as follows.

1. No effect of confinement is observed as regards capacity to store volumetric elastic strain energy, although the concrete experiences micro-cracks which causes mechanical defects if the hydrostatic stresses is less than 60% of the uniaxial compressive strength.
2. The capacity to store shear elastic strain energy is greatly influenced by the level of confinement applied to the concrete. Confinement reduces the rate of continuum fracturing when elastic strain increases.
3. There is a one-to-one relationship between the progress of deviatoric plastic strain and the deviatoric elastic strain, no matter what the level of confinement applied to the concrete. This means no effect of confinement is seen in the progress of deviatoric plasticity.
4. The confinement and level of concrete damage greatly affect the dilatancy, which relates to the volumetric plastic strain due to shear plastic strain. Confinement reduces the progress of dilatancy. On the other hand, continuum fracturing in the concrete explicitly increases dilatancy.

Experimental verifications were carried out for the case of steel-encased cylinders, and stress-strain, failure envelopes and loading paths and strain responses were computed. The versatility of proposed model was proven.

ACKNOWLEDGMENT : The authors are grateful for the valuable advice given by Prof. H. Okamura of the University of Tokyo and for the experimental help given by Mr. J. R. Khan of the Asian Institute of Technology. The first author is grateful to the Japan International Cooperation Agency for its financial support when the author served at Asian Institute of Technology. This study was conducted with Grant-in-Aid for Scientific Research No. 04555114 from the Ministry of Education, Science and Culture.

REFERENCES

1) Maekawa, K. and Okamura, H., The Deformational Behavior and Constitutive Equations for Concrete Using Elasto-Plastic and Fracture Model, *Journal of the Faculty of Engineering*, The University of Tokyo (B), Vol.XXXVII, No.2, 1983, pp.253-328

2) Maekawa, K. and Li, B., Elasticity and Plasticity of Concrete under Principal Stress Rotation, *Finite Element Analysis of Reinforced Concrete Structures*, Meyer, C. and Okamura, H. (Editors), ASCE, 1985, pp.72-92

3) Song, C. M., Maekawa, K., and Okamura, H., Time and Path-dependent Uniaxial Constitutive Model of Concrete, *Journal of the Faculty of Engineering*, The University of Tokyo (B), Vol.XLI, No.1, 1991, pp.159-237

4) Chen, W. F. and Saleeb, A. F., *Constitutive Equation for Engineering Materials*, Vol.1, John Wiley & Sons, 1981

5) Ohshima, M. and Hashimoto, C., Mechanical Properties of Concrete Confined by Steel Rings, *Summaries on the 39th Annual Convention*, Vol.V, Japan Society of Civil Engineers, 1984

6) Lorrain, M. and Loland, K. E., Damage Theory Applied to Concrete, *Fracture Mechanics of Concrete*, F.H. Wittmann (Editor), Elsevier Science Publishers, 1983

7) Kotsovos, M. D. and Newman, J. B., Generalized Stress-Strain Relations for Concrete, *Journal of the Engineering Mechanics*, ASCE, Vol.104, EM4, 1987

8) Eberhardsteiner, J., Meschike, G., and Mang, H. A., Triaxiales Konstitutives Modellieren Von Beton zum Zwecke der Durchfuhrung Vergleichender Traglastanalysen Dickwandiger Stahlbetonkonstruktionen Mittels der Methode der Finiten Elemente, *Institute for Strength of Materials,* Technical University of Vienna, Wien, 1987

9) Mazars, J. and Pijavdier-Cabot, G., Continuum Damage Theory: Application to Concrete, *Journal of Engineering Mechanics*, ASCE, Vol.115, 1989, pp.345-365

10) Takemura, J. and Irie, M., Constitutive Law of Concrete under Triaxial Compression, *Summaries on the 43th Annual Convention*, Vol.V, Japan Society of Civil Engineers, 1988

11) Mazars, J., Description of Micro and Macro-scale Damage of Concrete Structures, *Engineering Fracture Mechanics*, Vol.25, No.5/6, 1986, pp.729-737

12) Simo, J. C. and Ju, J. W., Strain and Stress Based Continuum Damage Models I, Formulation, *International Journal of Solids and Structures*, Vol.23, No.7, pp.841-869

13) Schreyer, H. L. and Wang, M. L., Elementary Constitutive Relations for Quasi-Brittle Materials Based on Continuum Damage Mechanics, *Micro-mechanics of Failure of Quasi-Brittle Materials*, Shah, S. P. (Editor), Elsevier Pub., 1990, pp.95-104

14) Li, B., Maekawa, K. and Okamura, H., Contact Density Model for Cracks in Concrete, *Journal of the Faculty of Engineering*, The University of Tokyo (B), Vol.XL, No.1, 1989, pp.9-52

15) Chen, W. F., *Plasticity in Reinforced Concrete*, McGraw-Hill Book Company, Inc., New York, 1981

16) Pandle, G. N. and Zienkiewicz, O. C. (Editors), Soil Mechanics - Transient and Cyclic Loads, John Wiley & Sons, 1982

17) Kotsovos, M. D. and Newman, J. B., Mathematical Description of Deformational Behavior of Concrete under Complex Loading, *Magazine of Concrete Research*, Vol.31, No.107, June, 1979, pp.77-90

18) Maekawa, K., Song, C. M., and Irie, M., Unified Concept for Compressive Characteristics of Concrete - From 3D Confinement to Pre-cracking, *JCI Colloquium on Analytical Studies on Shear Design of Reinforced Concrete Structures*, Vol.JCI-C18, JCI, 1989, pp.31-38

19) Okamura, H. and Maekawa, K., Nonlinear Analysis and Constitutive Models of Reinforced Concrete, Gihodo-Syuppan, Tokyo, 1991

20) Sugano, T., Inoue, N., Koshika, N., Hironaka, Y., and Hayami, K., 3-Dimensional Nonlinear Analysis of Reinforced Concrete Columns under Repeated Bending and Shearing Forces, *Proceedings of JCI 2nd Colloquium on Shear Analysis of RC Structures*, Japan Concrete Institute, Vol.JCI-C5, October 1983, pp.87-96

21) Richart, F. E., Brandtzaeg, A., and Brown, R. L., A Study of the Failure of Concrete under Combined Compressive Stresses, University of Illinois, Engineering Experimental Station, *Bulletin* No.185, 1928, pp.104

22) Kotsovos, M. D. and Newman, J. B., Mathematical Description of Deformational Behavior of Concrete under Generalized Stress Beyond Ultimate Strength, *Journal of ACI*, Vol.77, No.5, October, 1980, pp.340-346

23) Balmer, G. G., Shearing Strength of Concrete under High Triaxial Stress - Computation of Mohr's Envelope as a Curve, Structural Research Laboratory Report No.SP-23, Bureau of Reclamation, United States Department of the Interior, 1949

24) Kupfer, H., Hilsdorf, H. K., and Rusch, H., Behavior of Concrete under Biaxial Stress, *Journal of ACI*, Vol.66, No.8, August 1969, pp.656-666

25) Ju, J. W., On Energy-Based Coupled Elasto-Plastic Damage Theories - Constitutive Modeling and Computational Aspects -, *Int. Journal of Solids and Structures*, Vol.25, 1989, pp.803-833

26) Bazant, Z. P. and Kim, S., Plastic Fracturing Theory for Concrete, *Journal of Engineering Mechanics*, ASCE, Vol.105, No.EM3, June, 1979

27) Research and Surveying Report on the Mechanical Properties of Concrete, Chapter 2, Constitutive Laws of Concrete, *Concrete Library*, No.69, JSCE, August, 1991

28) Committee Report on Ductility of Concrete Structures and Its Evaluation, Japan Concrete Institute, Vol.JCI-C12, March, 1988